JACS
JOURNAL OF THE AMERICAN CHEMICAL SOCIETY
Communication
pubs.acs.org/JACS

A General Strategy for the Discovery of Metabolic Pathways: D-Threitol, L-Threitol, and Erythritol Utilization in *Mycobacterium smegmatis*

Hua Huang,[†] Michael S. Carter,[†] Matthew W. Vetting,[§] Nawar Al-Obaidi,[§] Yury Patskovsky,[§] Steven C. Almo,[§] and John A. Gerlt*[,†,‡]

[†]Institute for Genomic Biology and [‡]Departments of Biochemistry and Chemistry, University of Illinois at Urbana−Champaign, Urbana, Illinois 61801, United States

[§]Department of Biochemistry, Albert Einstein College of Medicine, Bronx, New York 10461, United States

Supporting Information

ABSTRACT: We describe a general integrated bioinformatic and experimental strategy to discover the *in vitro* enzymatic activities and *in vivo* functions (metabolic pathways) of uncharacterized enzymes discovered in microbial genome projects using the ligand specificities of the solute binding proteins (SBPs) for ABC transporters. Using differential scanning fluorimetry, we determined that the SBP for an ABC transporter encoded by the genome of *Mycobacterium smegmatis* is stabilized by D-threitol. Using sequence similarity networks and genome neighborhood networks to guide selection of target proteins for pathway enzymes, we applied both *in vitro* and *in vivo* experimental approaches to discover novel pathways for catabolism of D-threitol, L-threitol, and erythritol.

With advances in sequencing technologies, the rate of discovery of novel proteins greatly exceeds the rate at which their functions can be established. A large fraction of proteins discovered in genome projects are misannotated because their functions are automatically assigned based on sequence homology. To solve this problem, large-scale approaches for functional assignment are needed. We recently described the use of sequence similarity networks (SSNs) and genome neighborhood networks (GNNs) to facilitate the assignment of functions to >85% of the members of the proline racemase superfamily.[1] SSNs allow large-scale visualization of sequence-function relationships in protein families and, with annotation information from the UniProt and other databases, identification of orthologous groups within the families. GNNs allow large-scale visualization of the genome contexts of isofunctional families, thereby facilitating identification of the components of metabolic pathways, including transport systems and transcriptional regulators as well as enzymes.

We also have demonstrated that the discovery of novel metabolic pathways can be guided by high-throughput ligand screening for the solute binding proteins (SBPs) of transport systems.[2] The substrates for catabolic pathways often are transported into cells using SBPs to deliver substrates to the permease components of transporters. Because genes encoding transport systems often are clustered with the genes encoding the catabolic pathway for the transported ligand, identifying the specificity of the SBP facilitates identification of the catabolic pathway. Here, we describe the use of these strategies to facilitate the discovery of novel catabolic pathways for all three tetritols, D-threitol, L-threitol, and erythritol, in *Mycobacterium smegmatis* mc^{2}155 (Figure 1).

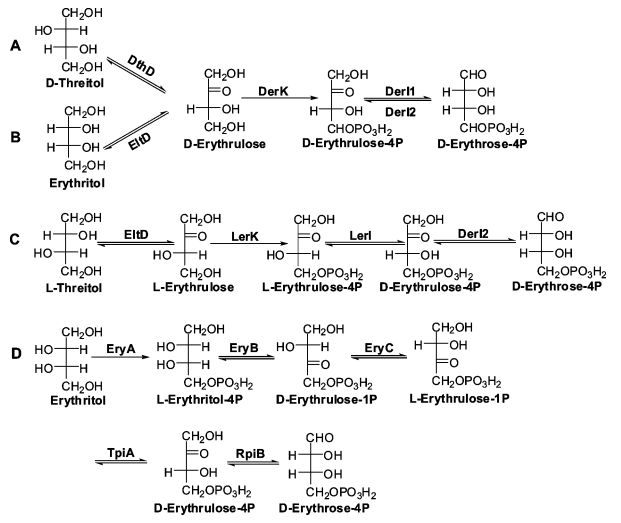

Figure 1. Tetritol catabolic pathways. (A) D-threitol catabolism in *M. smegmatis*; (B) erythritol catabolism in *M. smegmatis*; (C) L-threitol catabolism in *M. smegmatis*. Identifiers for the newly characterized enzymes in these pathways are summarized in Table S5; the relative locations of their genes are summarized in Figure 2. (D) Erythritol catabolism in *B. abortis*.[10]

The catabolic pathways for tetritols are not well-characterized.[3−5] The pathway for erythritol in *Brucella abortus*, which colonizes the placenta of cattle and sheep, was described recently;[6] the pathway is a virulence factor responsible for fetal abortions.[7,8] Erythritol is phosphorylated by EryA to yield L-erythritol-4P[9] that is converted to D-erythrose-4P, an intermediate of the pentose phosphate pathway by a dehydrogenase (EryB) and three isomerases (EryC, TpiA, RpiB; Figure 1D).[10]

Received: August 24, 2015
Published: November 11, 2015

DOI: 10.1021/jacs.5b08968
J. Am. Chem. Soc. 2015, 137, 14570−14573

Because its genome does not encode orthologues of these enzymes, *M. smegmatis* mc^{2}155 cannot utilize this pathway for erythritol catabolism.

Discovery of the pathways for all three tetritols in *M. smegmatis* mc^{2}155 was enabled by the ligand screen of SBPs for a large number of ABC transporters using differential scanning fluorimetry (DSF).[2] The screen identified two SBPs from *M. smegmatis* that (1) share 85% sequence identity, (2) are encoded by proximal genes, and (3) are stabilized by polyols (Figure S1). D-Threitol and xylitol stabilize MSMEG_3599 (ThpA, UniProt ID A0QYB5, PF134070, ΔT = 13−14.7 °C; see Table S5 for a summary of names and functions of SBPs/enzymes assigned in this study); xylitol, L-sorbitol, and L-sorbose stabilize MSMEG_3598 (XypA, UniProt ID A0QYB3, PF13407, ΔT = 12.6−13.6 °C). Structures for ThpA with D-threitol (PDB 4RSM) and for XypA with xylitol (PDB 4RS3) reveal a conserved polyol-binding site (Figure S2), except for the exchange of a Gln at residue 167 in ThpA for a Gly in XypA. The Gly produces a larger cavity that may explain the preference of XypA for the longer five- and six-carbon ligands.

The genome neighborhood of *xypA* and *thpA* (Figure 2A, Locus I) was examined to discover catabolic enzymes for their ligands. Four dehydrogenases are encoded by genes proximal to those encoding the SBPs. Based on their genome proximity, three of the dehydrogenases (MSMEG_3603, MSEG3604, and MSMEG_3605) may be encoded in one transcriptional unit; the gene for the fourth (MSEMG_3607) is divergently transcribed. Activities for oxidation of several polyols could be measured for three of the dehydrogenases (Table S6; MSMEG_3603 did not express as a soluble protein). MSMEG_3607 (DthD, UniProt ID A0QYC2, Pfam family PF00106) catalyzes the efficient oxidation of D-threitol (k_{cat}/K_m = 1.3×10^4 M^{-1} s^{-1}) that stabilizes ThpA, an SBP encoded in Locus I; this suggests that D-threitol is imported by ThpA before DthD catalyzes the first step in its catabolism. DthD does not catalyze the oxidation of the polyol ligands that stabilize XypA or the five- and six-carbon polyol ligands that stabilize ThpA. The specificity of DthD provides support for D-threitol as the physiological ligand for ThpA (and *vide infra*); the studies described here focus on discovery of the catabolic pathways for tetritols, including D-threitol, enabled by the ligand specificity of ThpA.

The suggested presence of a pathway for D-threitol catabolism prompted us to investigate whether *M. smegmatis* can utilize other tetritols. Immediate growth with D-threitol and erythritol was observed for wild-type *M. smegmatis*; growth with L-threitol was observed after a lag of nearly 60 h (Figure S3).

The genes that encode the catabolic pathways for all three tetritols are not proximal in the genome (*vide infra*), so they cannot be identified by inspection. Therefore, we used iterative analyses of SSNs and GNNs to identify the enzymes in the catabolic pathways for all three tetritols. Our discovery of the tetritol catabolic pathways provides a useful example of how large-scale analyses of protein sequence and genome context data can be used to discover novel metabolic pathways.

Initially we focused on D-threitol catabolism and generated SSNs and GNNs to identify the enzymes that catalyze the steps that follow DthD. First, the EFI-EST web tool (http://efi.igb.illinois.edu/efi-est/) was used to generate the SSN for the 2000 closest homologues of DthD in the UniProt database (Figure 3A).[11] Homologues in the SSN (highlighted in red in Figure 3A) include (1) an experimentally verified D-erythrulose reductase (Q8JIS3) from chicken liver that shares 37% identity to DthD;[5] and (2) an experimentally verified L-xylulose reductase from *M. smegmatis* (MSMEG_3262; UniProt ID A0QXD6; PDB 4EGF) that shares 44% identity to DthD.[12] These homologues of DthD

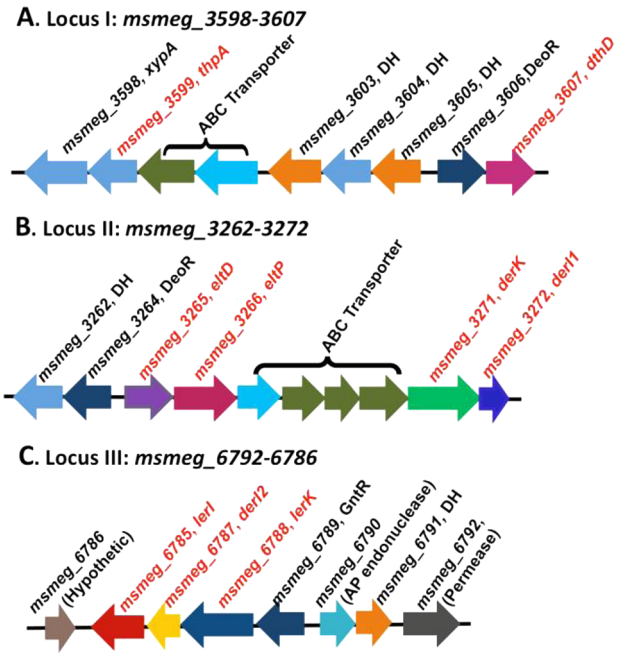

Figure 2. Genome neighborhoods that encode catabolic pathways for D-threitol, L-threitol, and erythritol. (A) Locus I (D-threitol transporter): the D-threitol transporter (*msmeg_3599*, *thpA*) and D-threitol dehydrogenase (*msmeg_3607*, *dthD*) are highlighted in red. (B) Locus II (D-erythrulose kinase): the D-eythrulose kinase (*msmeg_3271*, *derK*), D-erythrulose-4P isomerase (*msmeg_3272*, *derI1*), erythritol/L-threitol dehydrogenase (*msmeg_3265*, *eltD*), and the erythritol/L-threitol solute binding protein (*msmeg_3266*, *eltP*) are highlighted in red. (C) Locus III (L-erythrulose kinase): L-erythrulose kinase (*msmeg_6788*, *lerK*), L-erythrulose-4P epimerase (*msmeg_6785*, *lerI*), and D-erythrulose-4P isomerase (*msmeg_6787*, *derI2*) are highlighted in red. Abbreviation: DH, dehydrogenase.

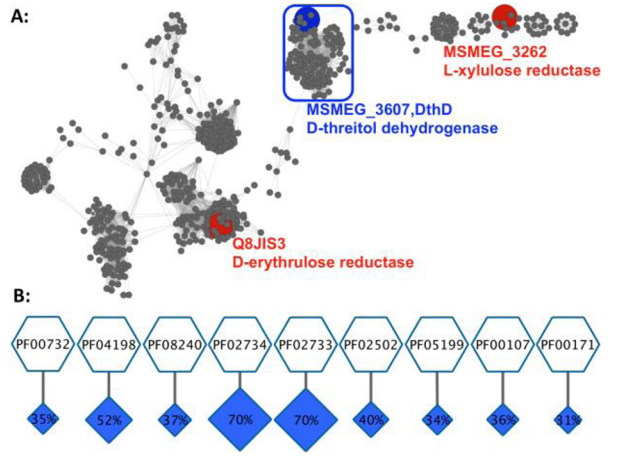

Figure 3. (A)SSN for the closest 2000 homologues of MSMEG_3607 (alignment score 60, 50% identity, 100% rep node network, singletons omitted). The nodes for characterized homologues are colored red, and the target enzyme is colored in blue. (B) GNN for the SSN cluster boxed in blue that allows the identification of D-erythrulose kinase and D-erythrulose-5P isomerase (PF02733, PF02734, and PF02502, respectively) in the catabolic pathway for D-threitol (co-occurrence frequencies are labeled in the blue spoke).

DOI: 10.1021/jacs.5b08968
J. Am. Chem. Soc. 2015, 137, 14570−14573

also catalyze the oxidation of alditols/reduction of ketoses. The alignment score (a measure of sequence similarity) used to generate the SSN in Figure 3A segregates the substrate specificities of homologues into different clusters, thereby identifying orthologues encoded by genomes of different species that may participate in the same pathways (see Materials and Methods in the Supporting Information for a detailed description of the procedures used to generate this and other SSNs as well as GNNs; these procedures are also described in refs 1 and 11).

Next, the EFI-GNT web tool (http://efi.igb.illinois.edu/efi-gnt/) was used to generate the GNN for the sequences in the SSN cluster that contains DthD in *M. smegmatis* and its orthologues in other species (Figure 3B); in this analysis the proteins encoded by the genes in a ±10 window relative to the genes encoding DthD and its orthologues are collected and partitioned into Pfam families. In the complete GNN provided by EFI-GNT, clusters are provided for the Pfam families of genome proximal enzymes, transport systems, and transcriptional regulators; the GNN in Figure 3B includes only the Pfam families for enzymes.

Genes that encode both subunits for dihydroxyacetone kinase (DaK1, PF02733 and DaK2, PF02734) co-occur with those encoding the sequences in the DthD SSN query cluster with a frequency of 70%, suggesting a role for a member of the dihydroxyacetone kinase family in the catabolism of D-threitol. However, the genome neighborhood of *dthD* in *M. smegmatis* (Figure 2A, Locus I) does not include genes for members of the DaK subunit families. Therefore, the SSN for the DaK1 family (PF02733) was generated (Figure S4) to identify members in *M. smegmatis*. Two proteins sharing 50% sequence identity were identified, MSMEG_3271 and MSMEG_6788. *In vitro* enzymatic assays established that MSMEG_3271 (DerK, UniProt ID A0QXE4) is a kinase specific for D-erythrulose and produces D-erythrulose-4P (k_{cat}/K_m = 6.3 × 10^5 M^{-1} s^{-1}, Table S6); MSMEG_6788 (LerK, UniProt ID A0R758) is a promiscuous kinase that has a preference for L-erythrulose and produces L-erythrulose-4P (k_{cat}/K_m = 6.0 × 10^5 M^{-1} s^{-1}, Table S6). The genome neighborhoods of *derK* and *lerK* are shown in Figure 2B (Locus II) and Figure 2C (Locus III), respectively. Thus, the synergistic use of the SSN for DthD and its orthologues to query their genome contexts using the EFI-GNT web tool allowed identification of two additional genome neighborhoods in *M. smegmatis* that encode enzymes in catabolic pathways for D-threitol and erythritol (Locus II, Figure 2B) as well as L-threitol (Locus III, Figure 2C).

The GNN in Figure 3B also identifies members of the LacAB_RpiB family (PF02502) whose genes co-occur with those encoding the sequences in the DthD SSN query cluster with a frequency of 40%. The gene encoding one member of this family is annotated as ribose-5P isomerase (MSMEG_3272, UniProt ID A0QXE5, PF02502) and is proximal to the gene encoding DerK (Figure 2B, Locus II); we determined that MSMEG_3272 catalyzes the isomerization of D-erythrulose-4P to D-erythrose-4P (DerI1; Figure S6). The gene encoding a second member (MSMEG_6787, UniProt ID A0R757, 72% sequence identity to MSMEG_3272,) also is annotated as ribose-5P isomerase and is encoded proximal to LerK, the L-erythrulose kinase (Figure 2C, Locus III); we determined that MSMEG_6787 (DerI2) also catalyzes the D-erythrulose-4P isomerase reaction (Figure S6). Again, the synergistic use of the SSN for DthD and its orthologues with the EFI-GNT web tool identified additional enzymes in the catabolic pathways for D-threitol and erythritol (Locus II, Figure 2B) as well as L-threitol (Locus III, Figure 2C).

With the experimentally verified *in vitro* activities of DthD, DerK, and DerI1 (D-threitol dehydrogenase, D-erythrulose kinase, and D-erythrulose-4P isomerase, respectively), an *in vitro* pathway can be proposed for the conversion of D-threitol to D-erythrose-4P, an intermediate in the pentose phosphate pathway (Figure 1A). In support of the physiological roles of the D-threitol binding SBP (ThpA) and the proposed pathway, transcript levels were measured by qRT-PCR for *thpA*, *dthD*, *derK*, *derI1*, and *derI2* in cells grown with D-threitol or glycerol; the genes were upregulated 4−25-fold during growth on D-threitol relative to growth on glycerol (Figure S7). To confirm that the SBP and enzymes are involved in catabolism of D-threitol, their genes were independently deleted. With the exceptions of the *derI1* and *derI2* single mutants, the mutant strains were defective for growth with D-threitol (Figure S8A). When the genes encoding both erythrulose-4P isomerases were deleted (*derI1* and *derI2*), the strain could not utilize D-threitol.

Because orthologues of DthD (Figure 3B) are encoded by genes proximal to those that encode DerK and DerI in other organisms, the SSN/GNN synergy permitted their identification (Figure 2A, Loci II and III) in *M. smegmatis*. This demonstration of the utility of the coupled use of SSNs and GNNs to identify complete metabolic pathways is further exemplified by the identification of the catabolic pathways for L-threitol and erythritol.

Because the gene cluster (Figure 2C, Locus III) that encodes LerK also encodes a DerI2, we hypothesized that Locus III is involved in L-threitol or erythritol metabolism. The protein annotated as triose phosphate isomerase (MSMEG_6785, UniProt ID A0R756, PF00121) catalyzes the conversion of L-erythrulose-4P to D-erythrulose-4P (LerI, Figure S6). Thus, the enzymes encoded by Locus III convert L-erythrulose to D-erythrose-4P. LerI is a member of PF00121, the triose phosphate isomerase family (Figure S9B). Thus, this analysis reveals that not all members of this family catalyze the well-studied 1,2-proton-transfer reaction that interconverts D-glyceraldhyde-3P and dihydroxyacetone phosphate in glycolysis, i.e., the active site structure can be modified to catalyze a 1,1-proton-transfer reaction using the homologous L-erythrulose-4P/D-erythrulose-4P substrate/product.

The source of the L-erythrulose substrate for LerK was determined by investigating the proteins encoded by additional genes in all three loci. Locus II (Figure 2B) includes a gene annotated to encode an arabinitol-phosphate dehydrogenase (EltD, MSMEG_3265, UniProt ID A0QXD8, PF08240 and PF00107). EltD catalyzes the oxidation of tetritols and pentitols (Table S6), including erythritol and L-threitol with values of k_{cat}/K_m = 5.6 × 10^3 and 6.2 × 10^3 M^{-1} s^{-1}, respectively.

EltD oxidizes erythritol to D-erythrulose (Figure S10A), which then can enter the D-erythrulose kinase pathway established for D-threitol catabolism (Figure 1B). In support of this assignment, transcripts for the genes in Locus II were upregulated 8−38-fold during growth on erythritol compared to growth on glycerol (Figure S7B); also deletion mutants of these genes were defective for growth with erythritol (Figure S8B). Thus, we conclude that the catabolism of erythritol by *M. smegmatis* proceeds via this pathway (Figure 1B).

EltD also catalyzes the oxidation of L-threitol to L-erythrulose (Figure S10B,C) to provide L-erythrulose for the pathway encoded by Locus III (Figure 2C). In a strain (HH001) adapted for immediate growth on L-threitol (see Materials and Methods in Supporting Information and Figure S2B for strain details), transcripts of *eltD* in Locus II are upregulated 13-fold during L-

DOI: 10.1021/jacs.5b08968
J. Am. Chem. Soc. 2015, 137, 14570−14573

threitol growth, and transcripts of all Locus III genes are constitutively elevated compared to wild-type levels (Figure S7D). Deletion of *eltD* or any catabolic genes in Locus III results in loss of the ability of HH001 to grow with L-threitol (Figure S8C). We conclude that the pathway in Figure 1C is the catabolic pathway for L-threitol, although the conditions required for expression of Locus III genes in wild-type *M. smegmatis* are unknown.

Transcripts for a third ABC SBP (MSMEG_3266, UniProt ID A0QXD9, PF01547), encoded by a gene proximal to the gene encoding EltD (Figure 2B, Locus II), are upregulated when *M. smegmatis* is grown with erythritol or when HH001 is grown with L-threitol. When *msmeg_3266* is deleted from the wild-type or HH001 strains, the resulting strains are defective for erythritol or L-threitol growth (Figures S8BC). Therefore, MSMEG_3266 (EltP) is predicted to be the SBP for transport of erythritol and L-threitol (recall that ThpA is the SBP for transport of D-threitol). Erythritol and L-threitol then are catabolized according to the pathways described above (Figure 1). With these *in vitro* and *in vivo* data, four pathways for tetritol catabolism now are known: D-threitol in *M. smegmatis* (Figure 1A); erythritol in *M. smegmatis* (Figure 1B); L-threitol in *M. smegmatis* (Figure 1C); and erythritol in *B. abortus*[10] (Figure 1D).

Considering their central roles in these pathways, erythritol kinase (*Brucella*-like erythritol catabolism), erythritol/L-threitol dehydrogenase (*Mycobacterium*-like erythritol catabolism), D-threitol dehydrogenase (D-threitol catabolism), erythritol/L-threitol dehydrogenase, and L-erythrulose-4P epimerase (L-threitol catabolism) can be used as pathway markers. Homologues were identified in their SSNs and used to explore the species distribution of the pathways (Figure S11). Two erythritol pathways exist in mutual exclusion (Figure S11A). The erythritol kinase pathway from *Brucella* is present primarily in the *Rhizobiales*; the erythritol dehydrogenase pathway is present in *Actinobacteria*, *Firmicutes*, and some *β*- and *γ*-*Proteobacteria* (*Burkholderiales*, *Serratia*, *Yersinia*, and *Providencia*). The D-threitol pathway often coexists with either of the erythritol catabolic pathways (Figure S11A). However, the complete L-threitol catabolic pathway is found only in a few strains (*Mycobacterium smegmatis* mc2 155, *Gracilibacillus halophilus* YIM-C55.5, *Asaia platycodi* SF2.1, *Rubelimicrobium mesophilus* DSM 19309, *Halomonas* sp. BJGMM-B45, *Dorea* sp. 5-2, and *Clostridium* sp. KLE 1755) (Figure S11B).

We have described a strategy for metabolic pathway discovery using synergistic bioinformatic analyses (SSNs and GNNs) and experimental approaches (high-throughput DSF for SBPs, *in vitro* enzymology, and *in vivo* phenotypes, genetics, and transcript analyses). Because functionally linked proteins often are encoded in gene clusters, the integrated SSN/GNN approach is a powerful method for visualizing protein families and gene clustering to predict metabolic pathways. Indeed, this approach allowed us to identify a genomically dispersed but functionally interconnected network for utilization of all three tetritols in *M. smegmatis*. We expect that this strategy is generally applicable to discover novel enzymes in novel microbial metabolic pathways.

■ ASSOCIATED CONTENT

Supporting Information

The Supporting Information is available free of charge on the ACS Publications website at DOI: 10.1021/jacs.5b08968.

Experimental details and data (PDF)

■ AUTHOR INFORMATION

Corresponding Author

*j-gerlt@illinois.edu

Notes

The authors declare no competing financial interest.

■ ACKNOWLEDGMENTS

This work was supported by a cooperative agreement from the National Institutes of Health (U54GM093342). This research used resources of the Advanced Photon Source, a U.S. Department of Energy (DOE) Office of Science User Facility operated for the DOE Office of Science by Argonne National Laboratory under contract no. DE-AC02-06CH11357. Use of the Lilly Research Laboratories Collaborative Access Team (LRL-CAT) beamline at Sector 31 of the Advanced Photon Source was provided by Eli Lilly Company, which operates the facility.

■ REFERENCES

(1) Zhao, S.; Sakai, A.; Zhang, X.; Vetting, M. W.; Kumar, R.; Hillerich, B.; San Francisco, B.; Solbiati, J.; Steves, A.; Brown, S.; Akiva, E.; Barber, A.; Seidel, R. D.; Babbitt, P. C.; Almo, S. C.; Gerlt, J. A.; Jacobson, M. P. *eLife* **2014**.

(2) Vetting, M. W.; Al-Obaidi, N.; Zhao, S.; San Francisco, B.; Kim, J.; Wichelecki, D. J.; Bouvier, J. T.; Solbiati, J. O.; Vu, H.; Zhang, X.; Rodionov, D. A.; Love, J. D.; Hillerich, B. S.; Seidel, R. D.; Quinn, R. J.; Osterman, A. L.; Cronan, J. E.; Jacobson, M. P.; Gerlt, J. A.; Almo, S. C. *Biochemistry* **2015**, *54*, 909.

(3) Hollmann, S.; Touster, O. *J. Biol. Chem.* **1957**, *225*, 87.

(4) Uehara, K.; Mannen, S.; Hosomi, S.; Miyashita, T. *J. Biochem.* **1980**, *87*, 47.

(5) Maeda, M.; Kaku, H.; Shimada, M.; Nishioka, T. *Protein Eng., Des. Sel.* **2002**, *15*, 611.

(6) Sangari, F. J.; Aguero, J.; Garcia-Lobo, J. M. *Microbiology (London, U. K.)* **2000**, *146*, 487.

(7) Anderson, J. D.; Smith, H. *J. Gen. Microbiol.* **1965**, *38*, 109.

(8) DelVecchio, V. G.; Kapatral, V.; Redkar, R. J.; Patra, G.; Mujer, C.; Los, T.; Ivanova, N.; Anderson, I.; Bhattacharyya, A.; Lykidis, A.; Reznik, G.; Jablonski, L.; Larsen, N.; D'Souza, M.; Bernal, A.; Mazur, M.; Goltsman, E.; Selkov, E.; Elzer, P. H.; Hagius, S.; O'Callaghan, D.; Letesson, J.-J.; Haselkorn, R.; Kyrpides, N.; Overbeek, R. *Proc. Natl. Acad. Sci. U. S. A.* **2002**, *99*, 443.

(9) Lillo, A. M.; Tetzlaff, C. N.; Sangari, F. J.; Cane, D. E. *Bioorg. Med. Chem. Lett.* **2003**, *13*, 737.

(10) Barbier, T.; Collard, F.; Zuniga-Ripa, A.; Moriyon, I.; Godard, T.; Becker, J.; Wittmann, C.; Van Schaftingen, E.; Letesson, J.-J. *Proc. Natl. Acad. Sci. U. S. A.* **2014**, *111*, 17815.

(11) Gerlt, J. A.; Bouvier, J. T.; Davidson, D. B.; Imker, H. J.; Sadkhin, B.; Slater, D. R.; Whalen, K. L. *Biochim. Biophys. Acta, Proteins Proteomics* **2015**, *1854*, 1019.

(12) Baugh, L.; Phan, I.; Begley, D. W.; Clifton, M. C.; Armour, B.; Dranow, D. M.; Taylor, B. M.; Muruthi, M. M.; Abendroth, J.; Fairman, J. W.; Fox, D.; Dieterich, S. H.; Staker, B. L.; Gardberg, A. S.; Choi, R.; Hewitt, S. N.; Napuli, A. J.; Myers, J.; Barret, L. K.; Zhang, Y.; Ferrell, M.; Mundt, E.; Thompkins, K.; Tran, N.; Lyons-Abbott, S.; Abramov, A.; Sekar, A.; Serbzhinskiy, D.; Lorimer, D.; Buchko, G. W.; Stacy, R.; Stewart, L. J.; Edwards, T. E.; Van Voorhis, W. C.; Myler, P. J. *Tuberculosis (Oxford, U. K.)* **2015**, *95*, 142.

DOI: 10.1021/jacs.5b08968
J. Am. Chem. Soc. 2015, 137, 14570−14573